JETP Letters, Vol. 80, No. 7, 2004, pp. 487–490. Translated from Pis'ma v Zhurnal Éksperimental'noĭ i Teoreticheskoĭ Fiziki, Vol. 80, No. 7, 2004, pp. 555–559.

Solid-State Synthesis in Ni/Fe/MgO(001) Epitaxial Thin Films

V. G. Myagkov[1, *], O. A. Bayukov[1], L. E. Bykova[1], V. S. Zhigalov[1], and G. N. Bondarenko[2]

[1] *Kirensky Institute of Physics, Siberian Division, Russian Academy of Sciences, Akademgorodok, Krasnoyarsk, 660036 Russia*

* *e-mail: miagkov@iph.krasn.ru*

[2] *Institute of Chemistry and Chemical Technology, Siberian Division, Russian Academy of Sciences, Krasnoyarsk, 660036 Russia*

Received June 27, 2004; in final form, August 16, 2004

Solid-state synthesis in Ni/Fe/MgO(001) bilayer epitaxial thin films has been studied experimentally. The phase sequence Fe/Ni $\longrightarrow$ (~350°C)Ni_3Fe $\longrightarrow$ (~400°C)NiFe $\longrightarrow$ (~550°C)γ_{par} is formed as the annealing temperature increases. The crystal structure in the invar region consists of epitaxially intergrown single-crystal blocks consisting of the paramagnetic γ_{par} and ferromagnetic NiFe phases, which satisfy the orientation relationship [100](001)NiFe || [100](001)γ_{par}. It has been shown that the nucleation temperatures of the Ni_3Fe, NiFe, and γ_{par} phases coincide with the temperatures of solid-state transformations in the Ni–Fe system. © *2004 MAIK "Nauka/Interperiodica".*

PACS numbers: 68.35.Rh; 68.55.Ac; 75.50.Bb

Iron–nickel alloys have been intensively studied for more than a century. The most striking feature of the Fe–Ni system with a high Fe concentration (C_{Fe} ~ 65 at. %) is a very low or even negative coefficient of thermal expansion. However, other physical characteristics, such as the Grüneisen parameter, elastic moduli, specific heats, magnetization, and resistivity also behave anomalously as functions of temperature, pressure, and magnetic field. These anomalous physical and magnetic properties are known as the invar problem [1]. The invar behavior has been observed for a number of iron alloys. The invar properties disappear above the Curie temperature, which indicates that the invar problem is associated with the existence of magnetic order in alloys. Most researches believe that the invar anomalies should be attributed to the existence of two electron spin states of iron in the γ phase. The first state is a low-spin γ_{LS} state with a small lattice constant (a ~ 0.355 nm). The second state is a ferromagnetic (high-spin γ_{HS}) state with a large lattice constant (a ~ 0.364 nm) [1]. According to theoretical calculations, γ iron and invar alloys with various lattice constants include many spin structures with very close energies (see [2, 3] and references cited therein) that are transformed to each other under varying temperatures and which can be responsible for the invar effect in the Fe–Ni system [3]. However, theoretical models are inconsistent with experimental data, where lattices with a > 0.36 nm for equilibrium γ phases of iron–nickel alloys have not yet been observed. Iron–nickel samples exhibiting the invar anomalies are metastable. Their transition to the equilibrium state is accompanied by the phase decomposition of the initial single γ-FeNi phase into a mixture of either γ and α phases in the process of low-temperature annealing or two γ phases for irradiated samples [1, 4–7]. The ordered (or partially ordered) ferromagnetic FeNi phase of the equiatomic composition is one of the γ phases, and the paramagnetic γ_{par} phase is the second γ phase [1, 4–7]. The paramagnetic γ_{par} phase is thought to be either the iron-rich FeNi phase or the Fe_3Ni phase [7, 8]. Mössbauer spectroscopy of iron–nickel alloys irradiated by fast electrons and invar meteorites (taenite) shows that two epitaxially intergrown γ phases with identical or close lattice constants exist at room temperature. These alloys do not undergo the γ $\longrightarrow$ α martensitic transformation and have no invar properties [1, 4, 5, 7].

The existence of the paramagnetic phase in iron–nickel alloys is well established. However, information is scarce about possible mechanisms of its formation, and data on the epitaxial relations with the FeNi phase are absent.

In this work, the formation of phases at the Fe/Ni interface under increasing annealing temperature and the conditions of formation of the paramagnetic γ_{par} phase in epitaxial Ni/Fe/MgO(001) thin films by solid-state synthesis are investigated.

Initial Ni/Fe/MgO(001) samples were obtained by the sequential vacuum deposition of iron and nickel layers on a freshly chipped MgO(001) surface. The thicknesses of iron and nickel films lay in the ranges 150–160 and 50–60 nm, respectively. This layer ratio ensured the formation of invar iron–nickel alloys after solid-state synthesis. To obtain epitaxial layers of iron and nickel, a substrate temperature of 250°C was kept during deposition. Figure 1a shows the diffraction pattern (CuK_α radiation) of the initial Ni/Fe/MgO(001)

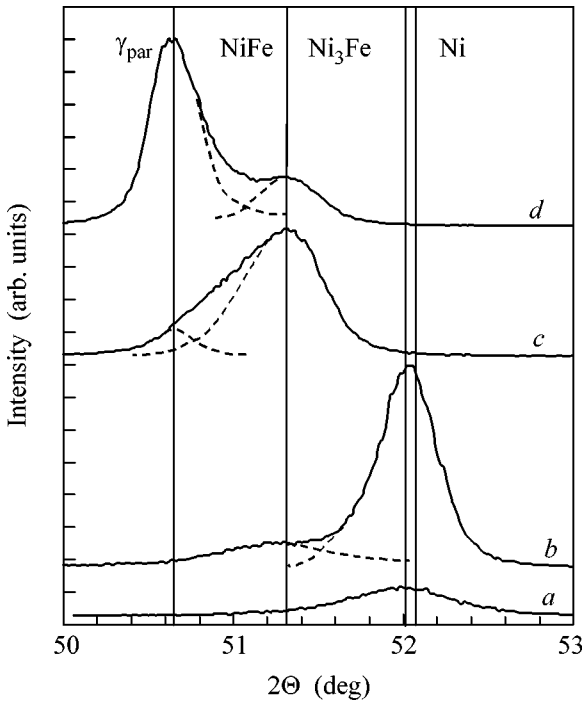

Fig. 1. Evolution of the (002) x-ray reflection of the γ phase in the Ni/Fe/MgO(001) sample during solid-state synthesis for various annealing temperatures: (*a*) initial sample, (*b*) 450, (*c*) 550, and (*d*) 800°C.

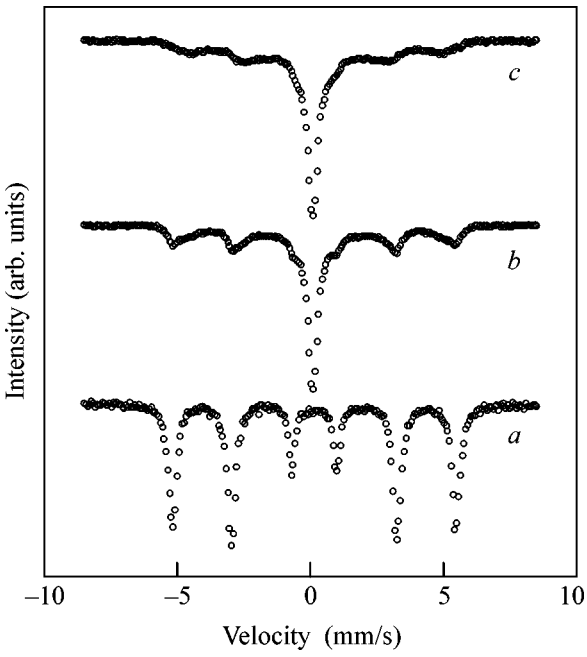

Fig. 2. ^{57}Fe Mössbauer spectra of the Ni/Fe/MgO(001) film sample after annealing at various temperatures: (*a*) initial sample, (*b*) 550, and (*c*) 800°C.

sample. This pattern includes only the Fe(002) and Ni(002) reflections and shows the epitaxial growth of the Fe(001) and Ni(001) layers on the MgO(001) surface under these deposition conditions. It is known that α-Fe and Ni epitaxial films grow on the MgO(001) surface with the maintenance of the orientation relationships [110](001)α-Fe ‖ [100](001)MgO [9, 10] and [100](001)Ni ‖ [100](001)MgO [10], respectively. Therefore, it should be expected that the initial Ni(001)/Fe(001)/MgO(001) samples have the same orientation relationships: [100](001)Ni ‖ [110](001)α-Fe ‖ [100](001)MgO. The Mössbauer spectra of the initial Ni(001)/Fe(001)/MgO(001) samples (Fig. 2a) involve lines in the ratio 3 : 4 : 1 and corroborate formation of α-Fe films on the MgO(001) substrate with the easy magnetization axis in the film plane.

The initial Ni(001)/Fe(001)/MgO(001) samples were subjected to temperature annealing through 50°C in the temperature range (300–700)°C during 30 min. Diffraction data show that the nickel film reacts completely at an annealing temperature of about 350°C, and that a new phase with a lattice constant $a = 0.3536$ nm is formed. Among stable intermetallic compounds, only the Ni_3Fe phase has a close lattice constant $a = 0.3545$ (JCPDS card 38-0419). However, epitaxial permalloy films with certain thicknesses may have a much smaller lattice constant $a = 0.3529$ nm [11]. This implies that Ni_3Fe is first formed at the interface of the Ni(001) and Fe(001) layers. The (002) reflection is single and strong and implies the epitaxial growth of the Ni_3Fe phase. The lattice constant close to the Ni lattice constant indicates that solid-state synthesis gives rise to the replacement of the Ni layer by the Ni_3Fe layer on the Fe(001) surface with the conservation of the orientation relationships [100](001)Ni_3Fe ‖ [110](001)α-Fe ‖ [100](001)MgO. An increase in the annealing temperature to ~400°C leads to formation of the NiFe phase with a lattice constant $a = 0.3568$ nm, which is slightly less than that in meteorite lamels [12]. The NiFe phase also grows epitaxially (Fig. 1b) between the Ni_3Fe(001) and Fe(001) layers. This growth of the NiFe phase on the Fe(001) surface corresponds to the orientation relationships [100](001)Ni_3Fe ‖ [100](001)NiFe ‖ [110](001)α-Fe ‖ [100](001)MgO. The Ni_3Fe phase disappears at an annealing temperature of about 500°C.

Formation of the Ni_3Fe and NiFe phases in the temperature range up to 550°C due to solid-state synthesis does not change the magnetization of the sample (Fig. 3), which is indicated by the additive contribution of the magnetic moments of iron and nickel atoms to the magnetization of the sample after the reaction. This magnetization lies on the Slater–Pauling curve. However, the magnetization of the sample drops sharply for a temperature of about 550°C (Fig. 3), which is associated with formation of a nonferromagnetic phase. The Mössbauer spectra also change and show that this phase is paramagnetic at room temperature (Fig. 2b). Diffraction reflections corroborate the formation of a

new phase with a lattice constant $a = 0.3600$ nm (Fig. 1c), which corresponds to an atomically disordered γ_{par} phase (taenite phase, JCPDS card 47-1417). The paramagnetic γ_{par} phase is a product of the solid-state synthesis of the residual iron layer in the NiFe phase. The γ_{par} phase, as well as the Ni_3Fe and NiFe phases, grows epitaxially (Fig. 1c) at the Fe(001)–NiFe(001) interface, satisfying the orientation relationships [100](001)NiFe ‖ [100](001)γ_{par} ‖ [100](001)MgO. Further annealing to a temperature of 800°C does not lead to formation of new phases, but the residual iron layer reacts completely, which increases the γ_{par} layer (Figs. 1d, 2c), and the NiFe(002) and γ_{par}(002) are clearly separated from each other (Fig. 1d).

An increase in the annealing time at a temperature of 700°C does not change the ratio of the intensities of the NiFe(002) and γ_{par}(002) diffraction peaks. Quenching from room temperature to liquid-nitrogen temperature is not accompanied by the martensitic transformation. The absence of rearrangements implies that [100](001)NiFe ‖ [100](001)γ_{par} epitaxially intergrown single-crystal blocks, which consist of the paramagnetic γ_{par} and ferromagnetic NiFe phases, are structurally stable in thin films over a wide temperature range. These samples are characterized by magnetocrystalline anisotropy with the constant $K_1 = -2.2 \times 10^4$ erg/cm^3 in the plane, which corroborates the epitaxial growth of the Ni_3Fe, NiFe, and γ_{par} phases in the process of solid-state synthesis. All Mössbauer spectra of these samples contain a sextet from the NiFe ferromagnetic phase and a paramagnetic singlet from the γ_{par} phase. Thus, the mechanism of the solid-state synthesis of intermetallides at the interface of the Fe(001) and Ni(001) single-crystal films may be as follows. Above 350°C, iron atoms begin to diffuse and discretely expand the nickel lattice with the sequential formation of the Ni_3Fe and NiFe phases. The further migration of iron atoms into the NiFe lattice at a temperature of about 550°C leads to the further expansion of the lattice, destruction of the ferromagnetic order in it, and formation of the γ_{par} phase. The above experimental data show that the two coherently intergrown γ phases obtained in this work are identical to the structure of irradiated iron–nickel alloys and invar meteorites [1, 4–8].

Numerous investigations have shown that a phase of reaction products, called the first phase, is formed in bilayer and multilayer films at a certain temperature upon heating. With a further increase in the annealing temperature, new phases, called phase sequences, are sequentially formed [13]. As was shown in [14–17], the initiation temperatures of solid-state reactions coincide with the temperatures of solid-state transformations of the reaction products. Indeed, solid-state synthesis in S/Fe bilayer films is initiated at the temperature of the metal–dielectric phase transition in iron monosulphide (FeS) [14]. The connection of solid-state synthesis with the order–disorder phase transition was investigated for

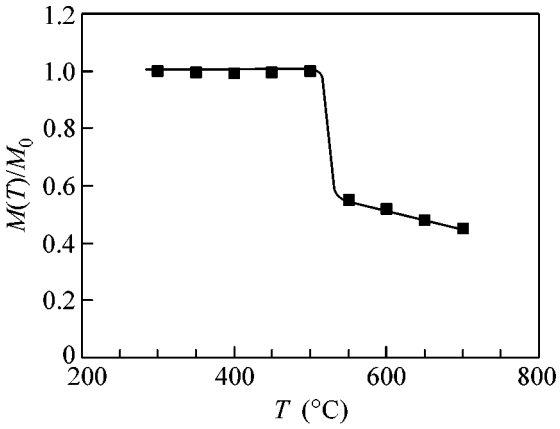

Fig. 3. Relative saturation magnetization of the Ni/Fe/MgO(001) film sample vs. annealing temperature.

the Cu–Au system, which is classical for the ordering phenomenon. Solid-state reactions in Cu/Au bilayer films proceed at the Kurnakov temperature of the CuAu superstructure formed in the reaction products [15]. It was shown in [16] that solid-state synthesis in Se/Cu bilayer films is associated with the superionic transition in copper selenide. Martensitic transformations are diffusionless solid-state transformations, wherein atoms pass from the austenite phase to the martensite phase by collective coherent motion without the rupture of chemical bonds. For this reason, it was surprising that compounds were formed at the temperature A_S of the reverse martensitic transformation [17].

According to the above analysis, solid-state synthesis in Fe/Ni bilayer films leads to formation of the phase sequence Fe/Ni $\longrightarrow$ (~350°C)Ni_3Fe $\longrightarrow$ (~400°C)NiFe $\longrightarrow$ (~550°C) γ_{par}. Therefore, the nucleation temperatures of the Ni_3Fe, NiFe, and γ_{par} phases must coincide with the temperatures of solid-state transformations of these phases. At present, reliable phase-transformation diagrams are absent for the Ni–Fe system. In the last variant of the state diagram for the Ni–Fe system, the temperature $T_0(Ni_3Fe) = 350$°C corresponds to the temperature (345°C) of eutectoid decomposition into a mixture of α-Fe and Ni_3Fe phases [18]. The temperature T_0(NiFe) = 400°C is close to the temperature (389°C) of the monotectic horizontal corresponding to decomposition into the paramagnetic and ferromagnetic phases [18]. The temperature $T_0(\gamma_{par}) = 550$°C must correspond to the temperature A_S of the inverse martensitic transformation. Experimental A_S values are absent for iron–nickel films and vary within the range (300–700)°C for bulk samples. The above comparison of the phase-nucleation temperatures with the temperatures of solid phase transformations in the Fe–Ni system is preliminary and requires further refinement.

Thus, it was shown that the phases Ni_3Fe ($a = 0.3536$ nm), NiFe ($a = 0.3568$ nm), and γ_{par} ($a =$

0.3600 nm) are sequentially formed at the interface of the Ni(001) and Fe(001) epitaxial layers as the annealing temperature increases. These phases are presumedly formed due to the migration of iron atoms into the nickel lattice with the conservation of the orientation relationships. The final products of solid-state synthesis are single-crystal blocks of the ferromagnetic NiFe and paramagnetic γ_{par} phases that are coherently intergrown and that have different lattice constants. An important conclusion is that the crystal structures of two γ phases intergrown due to solid-state synthesis in thin films, irradiated bulkiron–nickel alloys, and invar meteorites are identical.

This work was supported by the OAO MMK Foundation, the Research & Technological Centre Ausferr, and the Intels Foundation for Science and Education (project no. 10-03-02).

REFERENCES

1. V. L. Sedov, *Antiferromagnetism of Gamma Iron. The Invar Problem* (Nauka, Moscow, 1987) [in Russian].
2. V. P. Antropov, M. I. Katsnelson, M. van Schilfgaarde, and B. N. Harmon, Phys. Rev. Lett. **75**, 729 (1995); V. P. Antropov, M. I. Katsnelson, B. N. Harmon, *et al.*, Phys. Rev. B **54**, 1019 (1996); L. T. Kong and B. X. Liu, Appl. Phys. Lett. **84**, 3627 (2004).
3. M. van Schilfgaarde, I. A. Abricosov, and B. Johansson, Nature **400**, 46 (1999); Y. Wang, G. M. Stoks, D. M. C. Nicholson, and W. A. Shlton, J. Appl. Phys. **81**, 3873 (1997).
4. A. Chamberod, J. Laugier, and J. M. Penisson, J. Magn. Magn. Mater. **10**, 139 (1979).
5. J. Danon, R. B. Scorzelli, I. Souza-Azevedo, *et al.*, Nature **284**, 537 (1980).
6. S. S. Aliev, P. L. Gruzin, and A. Z. Men'shikov, Metallofizika (Kiev) **7**, 80 (1984).
7. D. G. Rancourt and R. B. Scorzelli, J. Magn. Magn. Mater. **150**, 30 (1995).
8. D. G. Rancourt, K. Lagarec, A. Densmore, *et al.*, J. Magn. Magn. Mater. **191**, 255 (1999).
9. G. Fahsold, A. Priebe, and A. Pucci, Appl. Phys. A **73**, 39 (2001).
10. S. Chikazumi, J. Appl. Phys. **32**, 81S (1961).
11. F. Michelini, J. Degauque, P. Baules, *et al.*, J. Magn. Magn. Mater. **242–245**, 173 (2002).
12. J. F. Albertsen, G. B. Jensen, and J. M. Knudsen, Nature **273**, 453 (1978).
13. *Thin Films: Interdiffusion and Reactions*, Ed. by J. M. Poate, K. N. Tu, and J. W. Mayer (Wiley, New York, 1978; Mir, Moscow, 1982); R. M. Walser and R. W. Bene, Appl. Phys. Lett. **28**, 624 (1976); R. W. Bene, Appl. Phys. Lett. **41**, 529 (1982); U. Gösele and K. N. Tu, J. Appl. Phys. **53**, 3252 (1982); J. Appl. Phys. **66**, 2619 (1989); F. M. d'Heurle and P. Gas, J. Mater. Res. **1**, 205 (1986); M. H. da Silva Bassani *et al.*, Scr. Mater. **37**, 227 (1997); J. J. Hoyt and L. N. Brush, J. Appl. Phys. **78**, 1589 (1995); W. H. Wang and W. K. Wang, J. Appl. Phys. **76**, 1578 (1994); M. Zhang, J. Appl. Phys. **80**, 1422 (1996); L. A. Clevenger, B. Arcot, W. Ziegler, *et al.*, J. Appl. Phys. **83**, 90 (1998); T. Nakanishi, M. Takeyama, A. Noya, and K. Sasaki, J. Appl. Phys. **77**, 948 (1995).
14. V. G. Myagkov, L. E. Bykova, G. N. Bondarenko, *et al.*, Dokl. Akad. Nauk **371**, 763 (2000) [Dokl. Phys. **45**, 157 (2000)].
15. V. G. Myagkov, L. E. Bykova, G. N. Bondarenko, *et al.*, Pis'ma Zh. Éksp. Teor. Fiz. **71**, 268 (2000) [JETP Lett. **71**, 183 (2000)].
16. V. G. Myagkov, L. E. Bykova, G. N. Bondarenko, *et al.*, Dokl. Akad. Nauk **390**, 35 (2003) [Dokl. Phys. **48**, 206 (2003)].
17. V. G. Myagkov, L. E. Bykova, L. A. Li, *et al.*, Dokl. Akad. Nauk **382**, 463 (2002) [Dokl. Phys. **47**, 95 (2002)]; V. G. Myagkov, L. E. Bykova, and G. N. Bondarenko, Dokl. Akad. Nauk **388**, 844 (2003) [Dokl. Phys. **48**, 30 (2003)]; V. G. Myagkov and L. E. Bykova, Dokl. Akad. Nauk **396**, 187 (2004) [Dokl. Phys. **49**, 289 (2004)].
18. *Phase Diagrams of Binary Metal Systems*, Ed. by N. P. Lyakishev (Mashinostroenie, Moscow, 1982), Vol. 2 [in Russian].

Translated by R. Tyapaev